

Construction of Response Patterns for Metal Cations by Using a Fluorescent Conjugated Polymer Sensor Array from Parallel Combinatorial Synthesis

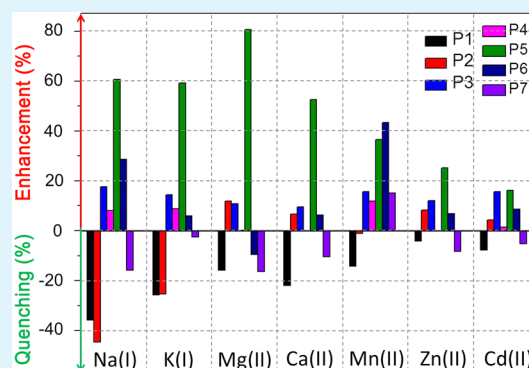
Haibo Xu, Wei Wu, Yun Chen, Tian Qiu, and Li-Juan Fan*

Jiangsu Key Laboratory of Advanced Functional Polymer Design and Application, Department of Polymer Science and Engineering, College of Chemistry, Chemical Engineering and Materials Science, Soochow University, Jiangsu, People's Republic of China, 215123

S Supporting Information

ABSTRACT: Pattern-based strategy is an emerging field of interest for effective sensing applications. Seven different conjugated polymers from combinatorial synthesis were combined into a sensor array, and seven metal cations were selected as representative analytes. The response patterns for each cation were constructed by collecting the individual fluorescence responses from seven polymers in the array. Each ion owns a characteristic pattern. Some of them have similar modes of response with subtle differences, while some patterns are distinctively different. The family/period the metal cations belong to and the charges/electronic configurations they possess may account for such similarity/difference in the pattern.

KEYWORDS: fluorescence, conjugated polymer, response pattern, sensor array, combinatorial synthesis



1. INTRODUCTION

There is great demand for developing new sensing materials and strategies for metal cations due to their ever increasing environmental and biological concern. Fluorescence-based methods are very desirable because of their sensitivity and simplicity.^{1–3} Conjugated polymers as fluorescent sensing materials offer distinct advantages, such as signal amplification and feasible structural modification.^{4–6} The conventional approach for construction of sensors usually follows the “lock-and-key” (one sensor to one analyte) paradigm. In most cases, the selectivity is achieved through the molecular recognition process based on shape/size match, host–guest/hydrophobic/electrostatic/dipole–dipole interaction, or π – π stacking between sensor and analyte. Sometimes, the mechanisms for signal transduction, such as cation-induced energy/electron transfer or aggregation/conformation variation of polymer chains, also play important roles. Though tremendous successful examples have been demonstrated using this conventional approach, some disadvantages cannot be ignored. High selectivity is preferred for each specific analyte, which requires the comprehensive consideration of all factors influencing the recognition and transduction process for the rational design of a sensory system. However, interference among analytes is common, which makes the realization of absolute selectivity difficult. Moreover, other interactions may also affect the sensing process to a certain degree, besides the predominant strong interaction between sensor and analyte. The actual sensing behaviors may deviate from the prediction. In addition, one separate sensor has to be fabricated for each

analyte, which inevitably requires a lot of work in the material preparation/optimization for different sensing needs.

Recently, an alternative pattern-based array sensing strategy is emerging that has been pioneered by several groups.^{7–29} A series of sensors are combined into an array. In such an array, each individual sensor responds differentially to many analytes, and a strict requirement for strong and selective affinity between the sensor and the specific analyte is unnecessary. Diverse sensors are included in this array to provide a characteristic response collection, which is called the response pattern or fingerprint, for each analyte. The “cross-interaction” between the sensor and analyte, which was deliberately avoided as much as possible in the conventional sensor approach, is used to generate a response pattern for different analytes. This pattern-based recognition, which actually is the basis of taste and olfactory sensation in human beings, has recently been used as “electronic nose/tongue” for analyzing the components of drinks, perfume, mixed solvents, and biomolecules.^{9,12,15,16} Only very few examples were about cation sensing,^{8,10,13} which were based on small molecule systems. The structural characteristics of conjugated polymers make the introduction of different types of the interactions with the analytes possible. They may have various interactions with cations in the side groups or backbone, and thus provide more differential responses than small molecular sensing molecules. However,

Received: January 7, 2014

Accepted: March 10, 2014

Published: March 10, 2014

there are only several reports^{22–29} using water-soluble conjugated polymers for bioanalyte detection based on pattern strategy, whereas no report for cation recognition, to our knowledge.

It is well-known that the synthesis of conjugated polymers is usually very time-consuming.^{30–33} The combinatorial synthesis, which has been widely used for effectively screening the right product in the drug synthesis, becomes a common tool for preparing sensing materials recently.^{34–37} Here, we present the efficient preparation of seven conjugated polymers, using combinatorial synthesis of different monomers (syntheses shown in Scheme 1) based on Sonogashira coupling (Scheme 2). The conjugated polymers differentiate from each other in the backbone or side group. Some of them have a poly[*p*-(phenyleneethynylene)-*alt*-(thienyleneethynylene)] (PPETE) backbone and some of them have a poly(*p*-phenyleneethynylene) (PPE) backbone. The side groups vary from the *N,N,N*-trimethylethane-1,2-diamino (tmeda), diethylamino (dea), alkoxy (OR), to ester-substituted alkoxy (ORCO₂R). Among these side groups, the tmeda side group has been demonstrated to have relatively strong chelating ability toward metal cations.^{38,39} Other side groups should have more or less interaction with the cations at the sites having O or N atoms. The delocalized electrons in the polymer backbone should also interact with the cations. In addition, the electron donating/withdrawing characteristics of side groups will affect the cation affinity of the polymer to various degrees. Therefore, the polymers with different combinations of backbones and side groups will have differential interactions with cations. Each polymer should give a response toward a cation, and the polymer array as an ensemble is expected to display various collective responses toward different cations. The response pattern for each cation thus can be constructed based on these collective responses. Such response patterns will be very useful for cation recognition through direct pattern-matching or further classification after data analysis with certain computational methods.

2. EXPERIMENTAL SECTION

2.1. Materials. 3-Methylthiophene, bis(trimethylsilyl)acetylene, bis(triphenylphosphine)palladium(II) chloride (PdCl₂(PPh₃)₂), tetrakis(triphenylphosphine)palladium ((PPh₃)₄Pd), and cuprous iodide (CuI) were purchased from Alfa Aesar Chemical Co. and used as received. Other commercially available reagents were from Sinopharm Chemical Reagent Co., Ltd. and were used without further purification unless otherwise noted. Tetrahydrofuran (THF) was dried by distillation from sodium metal and kept under argon. Triethylamine and diisopropylamine were distilled over potassium hydroxide before use.

2.2. General Methods. ¹H NMR spectra were recorded on an Inova 400 MHz NMR spectrometer with tetramethylsilane as the internal standard. The FTIR spectra of the monomers and polymers were obtained on a Nicolet 6700 FTIR spectrophotometer (thermo) with KBr pellets. Elemental microanalyses were carried out on a Carlo-Erba Elemental Analyzer EA 1110. Gel permeation chromatography (GPC) measurements were performed on a Waters 1515 system with THF as the mobile phase and polystyrene as the standard. For P1, P2 and P5, P6, triethylamine (8% in volume) was added in THF, during the preparation of the samples for GPC measurements, to reduce the interaction between the amino group and the column surface. The UV–vis absorption spectra were collected on a Hitachi U-3900/3900H spectrophotometer, and photoluminescence (PL) emission spectra were measured on a Horiba FluoroMax-4 spectrofluorometer using excitation at 440 nm. The polymer stock solutions were prepared as described previously.⁴⁰ The final concentration of the polymers for

the cation sensing experiment was held at 5 μM with respect to the repeating unit of the conjugated polymer backbone. All the cationic stock solutions were prepared by dissolving their chlorides in water. The titration of cations into the fluorescent solution was carried out by pipetting small aliquots of cation aqueous solution into 50 mL of polymer in THF solution to reach a desired cation concentration.³⁸ All the titrations were repeated at least three times, and the data were very reproducible with negligible deviation. The fluorescence quantum yields in solution of the polymers were determined relative to quinine sulfate in 0.5 M H₂SO₄ solutions with a quantum yield of 0.546, excited at 365 nm.⁴¹

2.3. Synthesis of Monomers. *N*-(2,5-Dibromothiophen-3-ylmethyl)-*N,N,N'*-trimethylethane-1,2-diamine (M1), 2,5-dibromothiophen-3-ylmethyl-diethylamine (M2), 1,4-diido-2,5-didodecyloxybenzene (M3), and 1,4-diethynyl-2,5-didodecyloxybenzene (M5) were synthesized according to the published procedures.^{38,39,42–45} 2,5-Bis(dodecyloxycarbonylmethoxy)-1,4-dibromobenzene (M4) and 2,5-bis(dodecyloxycarbonylmethoxy)-1,4-diethynylbenzene (M6) were synthesized by a modification of the literature report.⁴⁴

2,5-Dibromohydroquinone. Hydroquinone (8.56 g, 77.8 mmol) dissolved in 43 mL of acetic acid was placed into a Schlenk flask, followed by the dropwise addition of 8 mL of bromine dissolved in 35 mL of acetic acid, over a period of 1 h. The reaction mixture was stirred overnight at 10 °C. The resulting solid after filtration was recrystallized over methanol/deionized water. The white crystals were collected and dried in vacuum over night. Yield 13.52 g (65%). ¹H NMR (400 MHz, DMSO, δ): 9.8 (s, 2H), 7.1 (s, 2H).

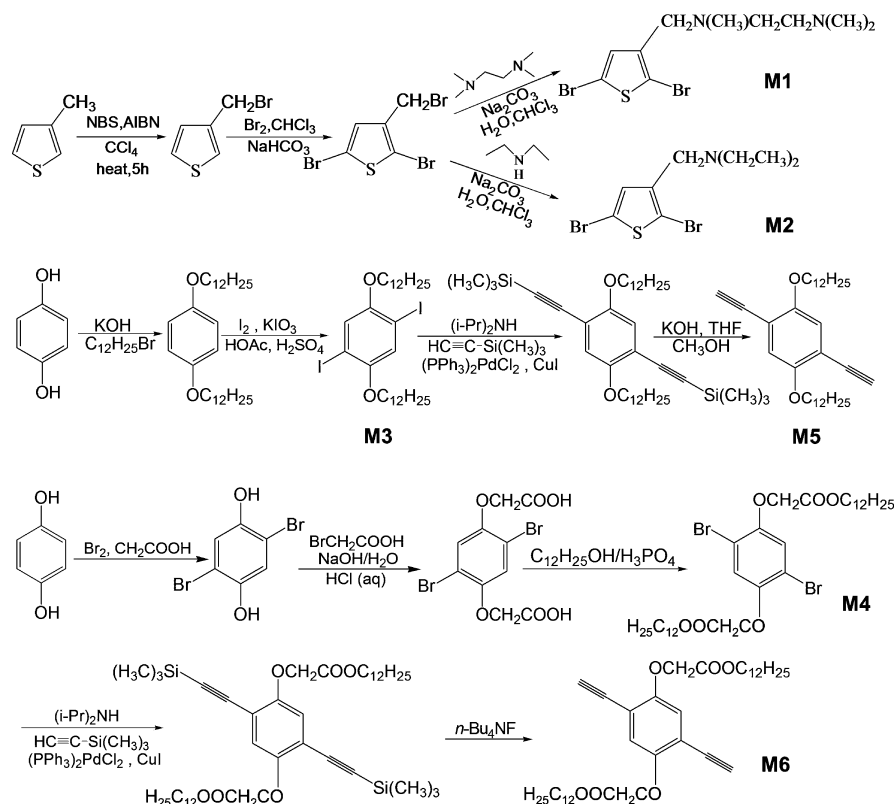
2,5-Bis(carboxymethoxy)-1,4-dibromobenzene. A mixture of 2,5-dibromohydroquinone (13.79 g, 51.5 mmol), bromoacetic acid (16.10 g, 115.9 mmol), and potassium carbonate (32.01 g) in 276 mL of ethanol was refluxed for 2 h, and then cooled down to room temperature. The solid was collected after filtration and washed with a small volume of cold water and cold ethanol to give a brown solid. Yield 14.21 g (72%). ¹H NMR (400 MHz, DMSO, δ): 13.1 (s, 2H), 7.2 (s, 2H), 4.7 (s, 4H).

2,5-Bis(dodecyloxycarbonylmethoxy)-1,4-dibromobenzene (M4). M4 was synthesized according to a modification of a literature report.⁴⁴ A 16.90 g (44.0 mmol) portion of 2,5-bis(carboxymethoxy)-1,4-dibromobenzene was added into a mixture of 156.00 g of *n*-dodecanol and 2.10 g of phosphoric acid, and refluxed for 6 h. After cooling down to room temperature, the reaction mixture was filtered. The resulting solid was recrystallized over ethyl acetate to give a white fine powder. Yield 18.69 g (61%). ¹H NMR (400 MHz, CDCl₃, δ): 7.09 (s, 2H), 4.6 (s, 4H), 4.2 (t, 4H), 1.7 (m, 4H), 1.3 (m, 36H), 0.9 (t, 6H).

2,5-Bis(dodecyloxycarbonylmethoxy)-1,4-di(trimethylsilyl)ethynylbenzene. 2,5-Bis(dodecyloxycarbonylmethoxy)-1,4-dibromobenzene (2.10 g, 3.0 mmol) was added to a mixture of CuI (0.0273 g, 0.14 mmol) and (PPh₃)₂PdCl₂ (0.0997 g, 0.14 mmol) in 41 mL of diisopropylamine, followed by the dropwise addition of trimethylsilylacetylene (3.00 g, 30 mmol) under an argon atmosphere. The mixture was stirred at room temperature for 1 h and refluxed for 2 h under argon, and then cooled down to room temperature. Toluene (30 mL) was added into the mixture. The filtrate was collected after the filtration. A brown solid was obtained after removing the solvent under reduced pressure. The solid was redissolved in 50 mL of toluene, and then purified through flash chromatography with a short silica gel column. A white solid was obtained after removing the solvent. The solid was recrystallized over chloroform/ethanol to give a white flaky solid. Yield 1.37 g (60%). ¹H NMR (400 MHz, CDCl₃, δ): 6.9 (s, 2H), 4.6 (s, 4H), 4.2 (t, 4H), 1.7(m, 4H), 1.3(m, 36H), 0.9(t, 6H), 0.3(s, 18H).

2,5-Bis(dodecyloxycarbonylmethoxy)-1,4-diethynylbenzene (M6). 2,5-Bis(dodecyloxycarbonylmethoxy)-1,4-di(trimethylsilyl)ethynylbenzene (1.20 g, 1.6 mmol) was dissolved in 39 mL of dioxane in a Schlenk flask, and then 5.8 mL of 1 M *n*-Bu₄NF solution in THF was added. The solution was stirred for 30 min at room temperature. Then the solution was heated to 55 °C and kept under this temperature for 5 min. Afterward, water was added dropwise until a suspension appeared in the system. The resulting suspension was

Scheme 1. Synthetic Strategies for Monomers



cooled down to room temperature and then was kept in the refrigerator overnight. After filtration, the solid product was chromatographed over petroleum ether/ethyl acetate (10:1) on a silica column. After removing the solvent, the resulting solid was recrystallized over chloroform/ethanol to give a white solid. Yield 0.57 g (59 %). ¹H NMR (400 MHz, CDCl₃, δ): 6.9 (s, 2H), 4.6 (s, 4H), 4.2 (t, 4H), 3.4 (s, 2H), 1.7 (m, 4H), 1.3 (m, 36H), 0.9 (t, 6H).

2.4. Synthesis of Polymers. All the conjugated polymers (P1–P8, Table S1, Supporting Information) were synthesized with the similar procedure. P8 has exactly the same structure as that of P3 and will not be discussed in the following paragraph. The structures of P4,⁴⁴ P5,³⁸ P6,³⁸ and P7⁴⁶ have been reported previously and were synthesized similarly, with a modification to previous literature methods. The following are more details about the synthesis.

P1. A pre-dried Schlenk flask was charged with monomer M1 (0.356 g, 1.0 mmol), monomer M6 (0.611 g, 1.0 mmol), (PPh₃)₄Pd (58 mg, 0.050 mmol), and CuI (20 mg, 0.10 mmol). The flask was deoxygenated by several cycles of vacuum–argon cycling. Dry diisopropylamine (4 mL) and dry THF (20 mL) were quickly added into the flask under the protection of argon. The mixture was refluxed for 24 h under argon and then cooled to room temperature. Then chloroform (20 mL) was added into the reaction mixture. The mixture was washed twice with dilute NaHCO₃ solution and then deionized water. The organic layer was collected, and the solvent was removed under reduced pressure. The obtained solid was washed with hot water and hot methanol. The crude product was dissolved in chloroform and then precipitated in methanol twice. The final product was dried in vacuum for 24 h to give a reddish-orange solid (0.664 g, yield 85%). ¹H NMR (400 MHz, CDCl₃, δ): 6.8–7.2 (3H), 4.6–4.8 (4H), 4.2–4.3 (4H), 3.4–3.7 (2H), 2.3–2.6 (4H), 2.1–2.3 (9H), 0.8–1.9 (46H). UV–vis λ_{max}: 444 nm. Emission λ_{max}: 489 nm. FTIR: the formation of internal ethynyl link was confirmed by the presence of the 2194 cm⁻¹ stretch. Anal. Calcd for C₄₆H₇₂O₆N₂S (%): C, 70.73; H, 9.29; N, 3.586. Found: C, 67.74; H, 8.95; N, 2.67.

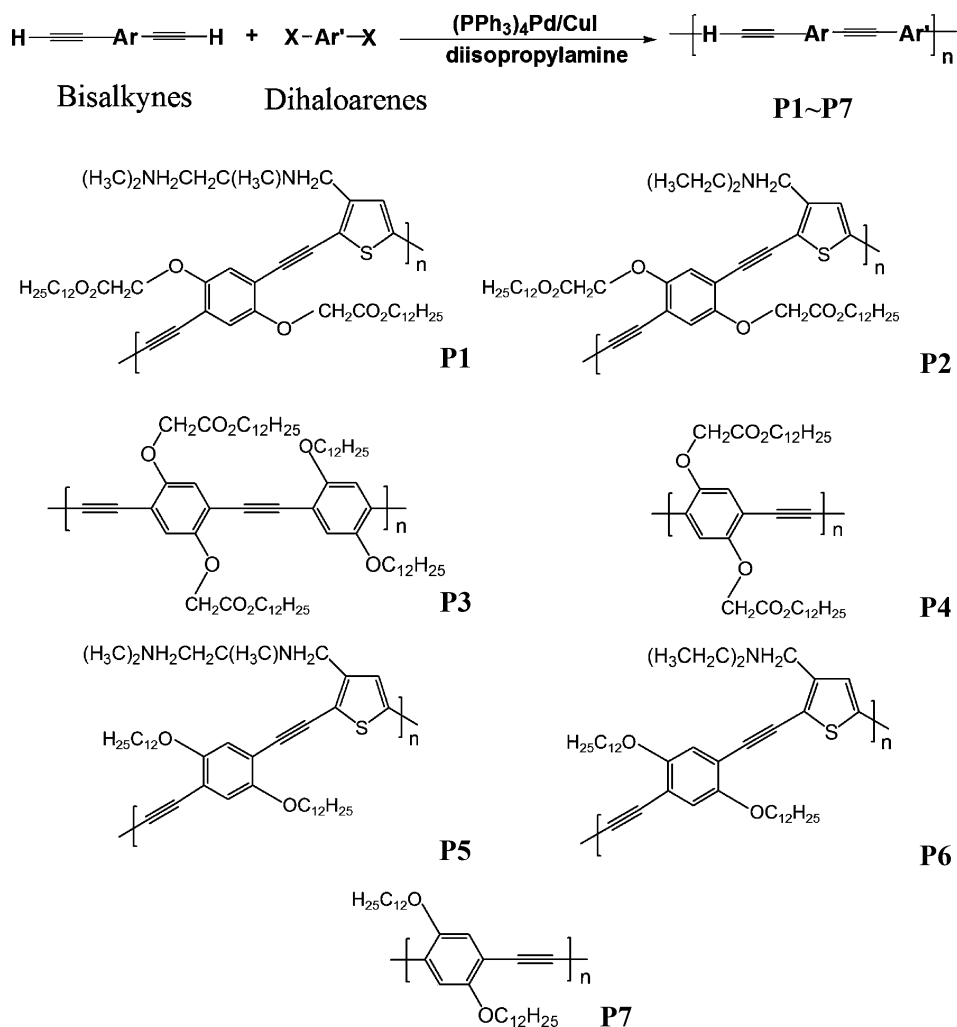
P2. A pre-dried Schlenk flask was charged with monomer M2 (0.327 g, 1.0 mmol), monomer M6 (0.611 g, 1.0 mmol), (PPh₃)₄Pd (58 mg, 0.050 mmol), and CuI (20 mg, 0.10 mmol). The flask was

deoxygenated by several cycles of vacuum–argon cycling. Dry diisopropylamine (4 mL) and dry THF (20 mL) were quickly added into the flask under the protection of argon. The mixture was refluxed for 24 h under argon and then cooled to room temperature. Then chloroform (20 mL) was added into the reaction mixture. The mixture was washed twice with dilute NaHCO₃ solution and then deionized water. The organic layer was collected, and the solvent was removed under reduced pressure. The obtained solid was washed with hot water and hot methanol. The crude product was dissolved in chloroform and then precipitated in methanol twice. The final product was dried in vacuum for 24 h to give a brown solid (0.654 g, yield 87%). ¹H NMR (400 MHz, CDCl₃, δ): 6.8–7.2 (3H), 4.6–4.8 (4H), 4.2–4.3 (4H), 3.4–3.7 (2H), 2.4–2.8 (4H), 0.8–1.8 (52H). UV–vis λ_{max}: 454 nm. Emission λ_{max}: 493 nm. FTIR: the formation of internal ethynyl link was confirmed by the presence of the 2193 cm⁻¹ stretch. Anal. Calcd for C₄₅H₆₉O₆NS (%): C, 71.86; H, 9.25; N, 1.86. Found: C, 75.03; H, 9.65; N, 0.67.

P3. A pre-dried Schlenk flask was charged with monomer M3 (0.494 g, 1.0 mmol), monomer M6 (0.611 g, 1.0 mmol), (PPh₃)₄Pd (58 mg, 0.050 mmol), and CuI (20 mg, 0.10 mmol). The flask was deoxygenated by several cycles of vacuum–argon cycling. Dry diisopropylamine (4 mL) and dry THF (20 mL) were quickly added into the flask under the protection of argon. The mixture was refluxed for 24 h under argon and then cooled to room temperature. The suspension was poured into 400 mL of cold methanol. Then the solid precipitated at the bottom was collected and dried in vacuum for 24 h to give a brown solid (0.813 g, yield 79%). ¹H NMR (400 MHz, CDCl₃, δ): 6.8–7.2 (4H), 4.5–4.8 (4H), 4.1–4.3 (4H), 3.8–4.1 (4H), 0.8–1.9 (92H). UV–vis λ_{max}: 439 nm. Emission λ_{max}: 472 nm. FTIR: the formation of internal ethynyl link was confirmed by the presence of the 2194 cm⁻¹ stretch. Anal. Calcd for C₆₆H₁₀₈O₈ (%): C, 77.00; H, 10.57. Found: C, 79.01; H, 10.33.

P4 (0.321 g, yield 56%). ¹H NMR (400 MHz, CDCl₃, δ): 6.8–7.2 (2H), 4.5–4.8 (4H), 4.1–4.3 (4H), 0.8–1.8 (46H). UV–vis λ_{max}: 435 nm. Emission λ_{max}: 466 nm. FTIR: the formation of internal ethynyl link was confirmed by the presence of the 2194 cm⁻¹ stretch. Anal. Calcd for C₃₅H₃₆O₆ (%): C, 73.39; H, 9.85. Found: C, 72.11; H, 9.77.

Scheme 2. Parallel Synthesis of Conjugated Polymers Using Sonogashira Proctol



P5 (0.552 g, yield 83%). ^1H NMR (400 MHz, CDCl_3 , δ): 6.8–7.2 (3H), 3.8–4.2 (4H), 3.4–3.7 (2H), 2.3–2.6 (4H), 2.1–2.3 (9H), 0.8–1.9 (46H). UV–vis λ_{max} : 454 nm. Emission λ_{max} : 493 nm. FTIR: the formation of internal ethynyl link was confirmed by the presence of the 2194 cm^{-1} stretch. Anal. Calcd for $\text{C}_{42}\text{H}_{68}\text{O}_2\text{N}_2\text{S}$ (%): C, 75.85; H, 10.31; N, 4.21. Found: C, 75.40; H, 9.53; N, 3.35.

P6 (0.515 g, yield 81%). ^1H NMR (400 MHz, CDCl_3 , δ): 6.8–7.2 (3H), 3.8–4.2 (4H), 3.4–3.7 (2H), 2.4–2.8 (4H), 0.8–2.0 (52H). UV–vis λ_{max} : 445 nm. Emission λ_{max} : 484 nm. FTIR: the formation of internal ethynyl link was confirmed by the presence of the 2194 cm^{-1} stretch. Anal. Calcd for $\text{C}_{41}\text{H}_{65}\text{O}_2\text{NS}$ (%): C, 77.43; H, 10.30; N, 2.20. Found: C, 77.81; H, 9.14; N, 1.77.

P7 (0.407 g, yield 89%). ^1H NMR (400 MHz, CDCl_3 , δ): 6.8–7.2 (2H), 3.8–4.2 (4H), 0.8–1.9 (46H). UV–vis λ_{max} : 422 nm. Emission λ_{max} : 470 nm. FTIR: the formation of internal ethynyl link was confirmed by the presence of the 2194 cm^{-1} stretch. Anal. Calcd for $\text{C}_{31}\text{H}_{52}\text{O}_2$ (%): C, 81.52; H, 11.48; N, 2.20. Found: C, 83.59; H, 11.16; N, 1.77.

3. RESULTS AND DISCUSSION

3.1. Synthesis and Characterization. The monomers were synthesized according to Scheme 1. Four dihaloarenes and two bisalkynes were obtained via three synthetic strategies. Some of them were synthesized exactly following literature descriptions. Some of them were synthesized by a modification of the literature methods, which were described in detail in the

Experimental Section. All the monomers were well characterized by ^1H NMR (Figure S1 in the Supporting Information).

Parallel polymerization under Sonogashira coupling protocol by combining the dihaloarenes and bisalkynes produced seven conjugated polymers with different structures (Scheme 2, and Table S1, Supporting Information). Some polymers have been reported previously, such as **P4**,⁴⁴ **P5**,³⁸ **P6**,³⁸ and **P7**.⁴⁶ Some are conjugated polymers with new structures, such as **P1**, **P2**, and **P3**, which have not been synthesized previously. There are two types of conjugated polymer backbones. **P1**, **P2**, **P5**, and **P6** have the poly[*p*-(phenyleneethynylene)-*alt*-(thienyleneethynylene)] (PPETE) backbone with amino pendant groups. **P3**, **P4**, and **P7** have the poly-(*p*-phenyleneethynylene) (PPE) backbone. The syntheses were carried out with the same amounts of reagents (in mole or volume) and under the same experimental conditions. It is to be noted that the volumes of the solvents (diisopropylamine and THF) were doubled comparing to the literature.³⁸ This change was based on the consideration of ensuring that the reaction intermediates were maintained in the dissolved state during the whole process of polymerization. It was observed that some of the polymer precipitated out of the reaction solution if using the exactly same amount of solvents as those in the literature. This polymerization based on Sonogashira coupling (Scheme 2) is a

step-growth polycondensation in principle; thus, a long polymerization time (24 h) is required.

All the resulting conjugated polymers are very soluble in common organic solvents, such as THF and chloroform. The polymers were well characterized by FTIR, NMR, GPC, and elemental analysis. The NMR spectra are shown in Figure 1. All

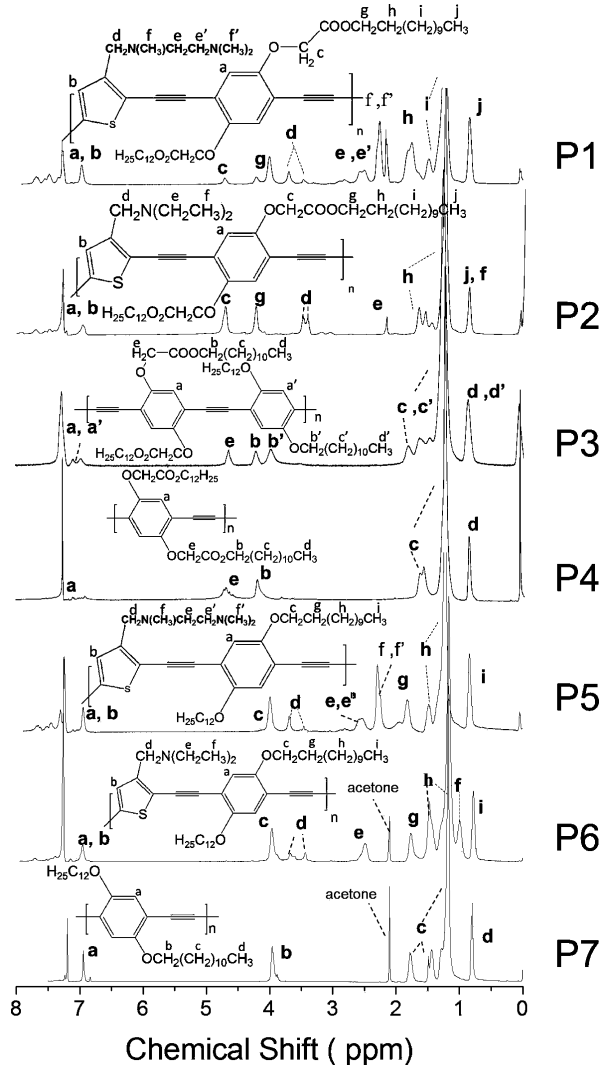


Figure 1. ^1H NMR spectra of the polymers (in CDCl_3).

the related peaks for the corresponding protons have been marked out. Generally, the C–H end groups of these polymers were below the signal-to-noise ratio in ^1H NMR, indicating the formation of polymer. In some cases, there are some peaks for the protons connected to the same carbon split into multiplets (marked as proton d in spectra for P1, P2, P5, and P6), which can be attributed to the regioisomerism of the protons in different electronic environments. Similar phenomena had also been reported and discussed in detail previously.³⁸ Both IR spectra (Figure S2 in the Supporting Information) and elemental analysis of the polymers are consistent with the desired structure. The molecular weights of the polymers were measured through GPC with polystyrene as the standard, and the results are shown in Table 1. Generally, the number average molecular weights (\overline{M}_n) fall in between 7500 and 15 000. Most polydispersity indexes (PDI) are around 2.00, which is an ideal value for a typical condensation polymerization. Using a flexible

Table 1. GPC and Photophysical Data for the Polymers

polymer	\overline{M}_w ($\times 10^4$)	\overline{M}_n ($\times 10^3$)	PDI	\overline{X}_n	$\lambda_{\text{max,abs}}$ (nm)	$\lambda_{\text{max,em}}$ (nm)	ϕ_f
P1	1.98	9.58	2.07	24	444	489	0.06
P2	1.86	9.33	1.99	24	454	494	0.10
P3	4.14	15.26	2.71	29	439	472	0.24
P4	1.32	7.65	1.72	26	435	466	0.22
P5	2.36	8.54	2.76	25	454	493	0.09
P6	1.66	7.80	2.13	24	445	484	0.11
P7	1.57	7.51	2.09	32	422	470	0.22

polystyrene standard may result in the overestimation of the \overline{M}_n for the rigid conjugated polymers.^{30,38,39} However, possible interaction exists between the columns and the polymers, especially those with amino pendant groups, such as P1, P2, P5, and P6.³⁸ Such interaction may prolong the eluent time of the polymers, and thus result in the underestimation of \overline{M}_n .^{30,38,39} These two influencing factors may cancel with each other. The degree of polymerizations (\overline{X}_n) calculated according to \overline{M}_n ranged from 24 to 32. Actually, such \overline{X}_n values for conjugated polymers, which even may be somewhat overestimated, not only ensured them to possess good solubility but also maintained the “molecular wire” effect to a certain degree.

3.2. Photophysical Properties. These polymers have typical absorption and emission spectra of conjugated polymers (Figure 2). The photophysical data are also shown in Table 1.

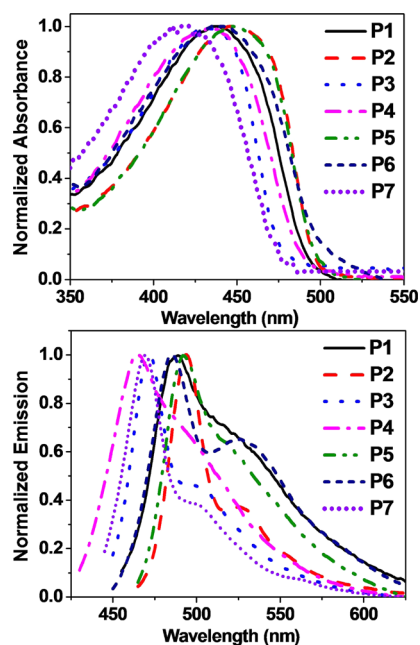


Figure 2. Absorption (up) and emission spectra (bottom) of conjugated polymers in THF solution at room temperature.

All the polymers displayed a broad absorption between 350 and 500 nm. The emission spectra are between 425 and 600 nm, having a peak at the shorter wavelength, accompanying with a shoulder at a relatively longer wavelength due to the vibronic structure. Generally, absorbance/emission peaks of the PPEs (P3, P4, P7) locate at shorter wavelengths than those of PPETEs (P1, P2, P5, P6), which are consistent with the literature for both types of conjugated polymers.^{38,40,46,47} This difference can be mainly attributed to the different electronic

band gaps that are dependent on the chemical structures of the polymers. The quantum yields of fluorescence (ϕ_f) were measured three times with a deviation $\leq \pm 0.01$. Comparing to PPEs, PPETEs (P1, P2, P6, P5) have smaller ϕ_f . This can be attributed to the partial fluorescence quenching due to the photoinduced electron transfer (PET) from the amino group to the polymer backbone, which inhibits the normal radiative decay of the excited state.^{38,39}

3.3. Cation Titration and Pattern Generation. Seven metal ions (Na^+ , K^+ , Mg^{2+} , Ca^{2+} , Mn^{2+} , Zn^{2+} , Cd^{2+}) were selected as representative analytes in this study. For comparison, they were typical monovalent/divalent cations from periods 3–5, differing in size, charge, or electron configuration (Table S2, Supporting Information). The cation titrations were carried out the same as those in previous studies.^{38,40} All the measurements were carried out three times, and negligible variations were found. The average values of fluorescence intensity changing (I/I_0) at the emission maximum versus the cation concentration (Figure S3, Supporting Information) was used for the analysis. The cation concentration was in the range of 0.125–10 μM .

Some general information for the cation sensing can be obtained from Figure S3 (Supporting Information). All the cations, more or less, enhanced the fluorescence of P5, which is consistent with the previous reports,³⁸ where the original design of P5 is as a fluorescence “turn-on” chemosensor based on photoinduced electron transfer. The lone electron pair on the amino group in P5 quenched the fluorescence from the polymer backbone. The chelation of metal cation lowered down the energy level of the electron pair on the nitrogen and thus restored the fluorescence. However, in the case of P6, the chelation induced enhanced fluorescence (CHEF) was not as effective as that with P5 since the diethylamino group is not a strong chelating group. Thus, less enhancing was observed, and even a small degree of quenching was observed for some cations at higher concentration for P6. Interestingly, P1, having the same amino pendant group as P5, but different neighboring side chains, displayed a fluorescence-quenching effect toward most metal cations. Some cations enhanced and some quenched the fluorescence in the cases of P2, P4, and P7, while all the cations slightly, but unanimously, enhanced the fluorescence of P3. It is to be noted that the difference in the chemical structure of the polymers should account for such a difference in the fluorescence response upon cations, while a detailed investigation into the mechanism has not been carried out since it is not a key interest of this study. Generally, it is not easy to distinguish different cations for most polymers if used individually, though each polymer solution has responses toward most cations. The lack of specificity is likely due to the cross interaction between most analytes and sensors in the array.

The main advantage for pattern-based analysis is that there is no strict requirement for high specificity, which might provide a cost-effective alternative method for sensing application comparing to the conventional strategy. The response pattern for each cation was constructed by collecting the individual response (intensity change, quenching or enhancing, at the emission peak) of each polymer solution upon 2 μM of analyte. The concentration of 2 μM was selected since the response for most cations reached the maximum around this concentration. The corresponding emission spectra are shown in Figure S4 (Supporting Information). All the resulting response patterns for the seven cations are summarized in Figure 3. The response

patterns upon 5 μM of analytes are also provided as Figure S5 (Supporting Information) for comparison.

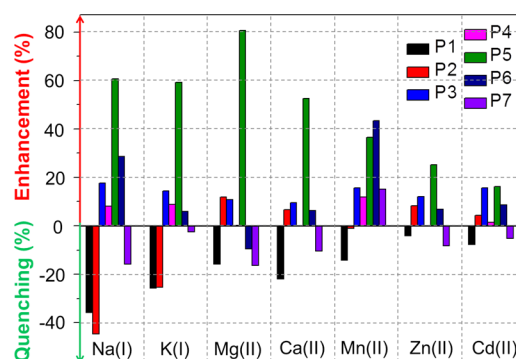


Figure 3. Response patterns for different metal ions constructed based on fluorescence responses of seven polymers upon 2 μM of cations. The percentages for extent of enhancement or quenching were calculated according to $(I/I_0 - 1) \times 100\%$ or $(1 - I_0/I) \times 100\%$, respectively.

Several general trends can be found after examining the response patterns for all the cations tested as a whole. First, metal ions from the same family have the similar pattern with slight differences. Na^+ and K^+ as representatives of IA group metal cations, both quenched the fluorescence of P1, P2, and P7, and enhanced the fluorescence of P3, P4, P5, and P6, while the extents of quenching/enhancing are different between these two cations. Mg^{2+} and Ca^{2+} from the IIA group displayed a very similar effect on the fluorescence of P1, P2, P3, P4, P5, and P7, whereas they have the opposite effect on the emission of P6. As for Zn^{2+} and Cd^{2+} from the IIB group, they have similar response patterns while the quenching or enhancing factors for each polymer are slightly different. Second, the patterns for metal ions from the same period, but different families, such as K^+ , Ca^{2+} , and Mn^{2+} , are found to be very different. Zn^{2+} seems to have a similar quenching/enhancing response as Ca^{2+} towards each polymer. However, the intensity changes of P1, P5, and P7 upon Zn^{2+} are smaller than those upon Ca^{2+} , whereas those of P2, P3, and P6 are larger, which makes it not difficult to discriminate between these two cations. Such similarity/difference in the response can be attributed to the differential interaction between cation and polymer. The characteristics of the cations (Table S2, Supporting Information), such as the family/period the metal cations belong to and the various charges/electronic configuration they have, should have great influence on the interaction with polymers and, therefore, the response patterns. Mn^{2+} displayed a most different pattern from other cations since it is the only cation with a half-filled 3d orbital; $\text{Mg}^{2+}/\text{Ca}^{2+}$ differ from Na^+/K^+ in the charge; $\text{Zn}^{2+}/\text{Cd}^{2+}$ have an additional p orbital and a larger size compared to $\text{Mg}^{2+}/\text{Ca}^{2+}$ at the same period, which might account for their smaller response from polymers with tmeda groups, due to the weaker chelation. In addition, the small difference in the pattern between the cations in the same family is very likely due to the different sizes they have.

One concern for the cation recognition is that if the pattern changes with the concentration. Comparing Figure 3 with Figure S5 (Supporting Information), no significant difference between the two concentrations of 2 and 5 μM can be found. To further explore the influence from the cation concentration, the response patterns for 13 concentrations tested (among

0.125–10 μM) were constructed for each cation. Patterns for Na^+ and Mn^{2+} , as representative cases, are shown in Figure 4,

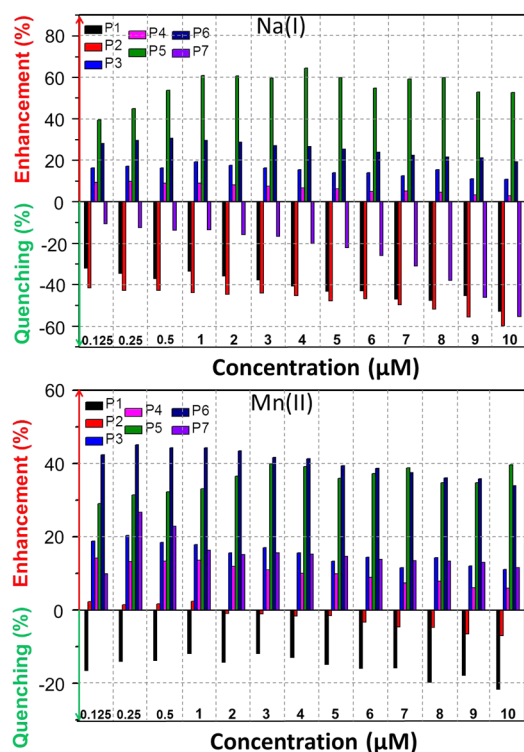


Figure 4. Response patterns for Na^+ (top) and Mn^{2+} (bottom) in different concentrations, constructed based on fluorescence responses of seven polymers. The percentages for extent of enhancement or quenching were calculated according to $(I/I_0 - 1) \times 100\%$ or $(1 - I_0/I) \times 100\%$, respectively.

and the others are shown in Figure S6 (Supporting Information). It can be seen that each metal cation produced a unique pattern, and the general appearance almost stayed the same, with nearly 2 orders of magnitude variation in the concentration. For each cation, most polymers displayed no significant difference in response upon different concentrations. Only a few polymers have changes in the extent of fluorescence enhancing/quenching with the increase of concentration of cations, which does not affect the response pattern of the cation in the general. On the other hand, such a difference can be used to identify the concentration of the cation, with those almost unchanged responses as the “inner standards”.

It is to be noted that sensitivity and limit of detection, which used to be the major performance indexes of conventional sensing systems, have not been mentioned in our study. We have not found any discussion about the sensitivity in the pattern/array-based sensing systems, to our knowledge. The possible reason may be that every sensor has a different sensitivity toward to an analyte, which makes it difficult to define the sensitivity of the whole array composed of many individual sensors. The measurements for the limit of detection have not been carried out since a tremendous amount work will be required for completing such measurements for all the systems. However, the limit of detection must be lower than 0.125 μM in our study, since the ion concentration range studied is between 0.125 and 10 μM .

The results above for the conjugated polymer sensor array demonstrated that such pattern-based analysis can be used for

the recognition of the family of metal cations. In addition, various cations in the same family can also be differentiated by the slight difference. For the sensing application in the real world, it is very practical to construct such response patterns using corresponding standard samples, and then identify the unknown analyte by comparing the patterns. Compared to the conventional method, the possible sacrifice for the reduced difficulty in the design and material preparation is the more complicated data matching or recognition procedure, which actually becomes more and more convenient with the increasingly powerful computer and information analysis techniques. With the aid of a computer, thousands of patterns can be stored in a database and the recognition of analytes can be achieved, simply by directly matching the patterns or further deconvolution of the data using some computational method.⁴⁸ The complete selectivity between the analyte and sensor rarely exists in the real application with the co-existence of many interferences, except the antigen–antibody interaction. The analyte of interest may exist in a mixture. This pattern-based strategy would be very advantageous for metal cation sensing in ruling out the misrecognition at the largest extent, by combining the various responses from several polymers having different types of interactions with one specific cation, instead of only one response from one sensor. Moreover, the possible fluorescent–intensity fluctuation during the measurements, which may be disadvantageous in obtaining the right information for the conventional method, will not affect the pattern-based sensing. With the aid of modern mathematic methods, such a pattern-based strategy should be advantageous in recognition of the analytes in a mixture, or with the presence of interferences. It is to be noted that various methods for computational analysis of such patterns have been well developed recently.⁴⁸ However, different methods applied to different systems, depending on the identities of the sensor arrays and the analytes. We believe that future deconvolution of the response pattern will give a much clearer classification of the analytes, but only based on choosing the right analysis method.

4. CONCLUSION

In conclusion, several different fluorescent conjugated polymers were efficiently synthesized using Sonogashira coupling by combining six monomers under the same reaction condition and were combined into a fluorescence sensor array. Photo-physical studies showed that the polymers displayed different, but typical, absorption and emission characteristics. Seven polymers showed various fluorescence responses upon cations in the cation titration experiment, which can be attributed to the differential interactions between cations and polymers. The collection of individual responses of seven polymer solutions in the presence of cations generated a characteristic and unique pattern for each cation. There is no large variation in the pattern appearance with respect to the concentration for each cation. Such patterns can be regarded as “fingerprints” for distinguishing different metal cations. The current study demonstrated that facile combinatorial synthesis of different building blocks endowed the resulting conjugated polymers with cross-interaction between conjugated polymers and cations, and, therefore, differential fluorescence responses in cation titration. Such a fluorescent conjugated polymer sensor array may provide new sensing opportunities with the pattern-based strategy, for those undetectable analytes by an individual

sensor. Moreover, the range of detectable analytes can also be expanded without increasing the synthetic difficulty.

■ ASSOCIATED CONTENT

■ Supporting Information

NMR, IR, and emission spectra, and some additional data. This material is available free of charge via the Internet at <http://pubs.acs.org>.

■ AUTHOR INFORMATION

■ Corresponding Author

*E-mail: ljfan@suda.edu.cn.

■ Notes

The authors declare no competing financial interest.

■ ACKNOWLEDGMENTS

The authors thank the National Natural Science Foundation of China (21174099, 21374071) and A Priority Academic Program Development of Jiangsu Higher Education Institutions (PAPD) for the financial support.

■ REFERENCES

- (1) de Silva, A. P.; Gunaratne, H. Q. N.; Gunnlaugsson, T.; Huxley, A. J. M.; McCoy, C. P.; Rademacher, J. T.; Rice, T. E. Signaling Recognition Events with Fluorescent Sensors and Switches. *Chem. Rev.* **1997**, *97*, 1515–1566.
- (2) Basabe-Desmonts, L.; Reinhoudt, D. N.; Crego-Calama, M. Design of Fluorescent Materials for Chemical Sensing. *Chem. Soc. Rev.* **2007**, *36*, 993–1017.
- (3) Ding, L.; Fang, Y. Chemically Assembled Monolayers of Fluorophores as Chemical Sensing Materials. *Chem. Soc. Rev.* **2010**, *39*, 4258–4273.
- (4) McQuade, D. T.; Pullen, A. E.; Swager, T. M. Conjugated Polymer-Based Chemical Sensors. *Chem. Rev.* **2000**, *100*, 2537–2574.
- (5) Thomas, S. W. I.; Joly, G. D.; Swager, T. M. Chemical Sensors Based on Amplifying Fluorescent Conjugated Polymers. *Chem. Rev.* **2007**, *107*, 1339–1386.
- (6) Fan, L. J.; Zhang, Y.; Murphy, C. B.; Angell, S. E.; Parker, M. F.; Flynn, B. R.; Jones, W. E., Jr. Fluorescent Conjugated Polymer Molecular Wire Chemosensors for Transition Metal Ion Recognition and Signaling. *Coord. Chem. Rev.* **2009**, *253*, 410–422.
- (7) Albert, K. J.; Lewis, N. S.; Schauer, C. L.; Sotzing, G. A.; Stitzel, S. E.; Vaid, T. P.; Walt, D. R. Cross-Reactive Chemical Sensor Arrays. *Chem. Rev.* **2000**, *100*, 2595–2626.
- (8) Goodey, A. P.; McDevitt, J. T. Multishell Microspheres with Integrated Chromatographic and Detection Layers for Use in Array Sensors. *J. Am. Chem. Soc.* **2003**, *125*, 2870–2871.
- (9) Stojanovic, M. N.; Green, E. G.; Semova, S.; Nikic, D. B.; Landry, D. W. Cross-Reactive Arrays Based on Three-Way Junctions. *J. Am. Chem. Soc.* **2003**, *125*, 6085–6089.
- (10) Basabe-Desmonts, L.; Beld, J.; Zimmerman, R. S.; Hernando, J.; Mela, P.; Garcia Parajo, M. F.; van Hulst, N. F.; van den Berg, A.; Reinhoudt, D. N.; Crego-Calama, M. A Simple Approach to Sensor Discovery and Fabrication on Self-Assembled Monolayers on Glass. *J. Am. Chem. Soc.* **2004**, *126*, 7293–7299.
- (11) Greene, N. T.; Shimizu, K. D. Colorimetric Molecularly Imprinted Polymer Sensor Array Using Dye Displacement. *J. Am. Chem. Soc.* **2005**, *127*, 5695–5700.
- (12) Wright, A. T.; Anslyn, E. V.; McDevitt, J. T. A Differential Array of Metalated Synthetic Receptors for the Analysis of Tripeptide Mixtures. *J. Am. Chem. Soc.* **2005**, *127*, 17405–17411.
- (13) Zimmerman, R.; Basabe-Desmonts, L.; van der Baan, F.; Reinhoudt, D. N.; Crego-Calama, M. A Combinatorial Approach to Surface-Confined Cation Sensors in Water. *J. Mater. Chem.* **2005**, *15*, 2772–2777.

(14) Wright, A. T.; Anslyn, E. V. Differential Receptor Arrays and Assays for Solution-Based Molecular Recognition. *Chem. Soc. Rev.* **2006**, *35*, 14–28.

(15) Edwards, N. Y.; Sager, T. W.; McDevitt, J. T.; Anslyn, E. V. Boronic Acid Based Peptidic Receptors for Pattern-Based Saccharide Sensing in Neutral Aqueous Media, an Application in Real-Life Samples. *J. Am. Chem. Soc.* **2007**, *129*, 13575–13583.

(16) Zhang, T.; Edwards, N. Y.; Bonizzoni, M.; Anslyn, E. V. The Use of Differential Receptors to Pattern Peptide Phosphorylation. *J. Am. Chem. Soc.* **2009**, *131*, 11976–11984.

(17) Severin, K. Pattern-Based Sensing with Simple Metal–Dye Complexes. *Curr. Opin. Chem. Biol.* **2010**, *14*, 737–742.

(18) Takeuchi, T.; Montenegro, J.; Hennig, A.; Matile, S. Pattern Generation with Synthetic Sensing Systems in Lipid Bilayer Membranes. *Chem. Sci.* **2011**, *2*, 303–307.

(19) Rout, B.; Unger, L.; Armony, G.; Iron, M. A.; Margulies, D. Medication Detection by a Combinatorial Fluorescent Molecular Sensor. *Angew. Chem., Int. Ed.* **2012**, *51*, 12477–12481.

(20) Kim, H.; Kwak, G. Combinatorially Responsive, Polarity-Indicative, Charge Transfer Dye-Based Polymer Gels for Odor Visualization in VOC Sensor Array. *Macromolecules* **2009**, *42*, 902–904.

(21) Röck, F.; Barsan, N.; Weimar, U. Electronic Nose: Current Status and Future Trends. *Chem. Rev.* **2008**, *108*, 705–725.

(22) Miranda, O. R.; You, C. C.; Phillips, R.; Kim, I. B.; Ghosh, P. S.; Bunz, U. H. F.; Rotello, V. M. Array-Based Sensing of Proteins Using Conjugated Polymers. *J. Am. Chem. Soc.* **2007**, *129*, 9856–9857.

(23) Zhu, C.; Yang, Q.; Liu, L.; Wang, S. Visual Optical Discrimination and Detection of Microbial Pathogens Based on Diverse Interactions of Conjugated Polyelectrolytes with Cells. *J. Mater. Chem.* **2011**, *21*, 7905–7912.

(24) Bajaj, A.; Miranda, O. R.; Phillips, R.; Kim, I.-B.; Jerry, D. J.; Bunz, U. H.; Rotello, V. M. Array-Based Sensing of Normal, Cancerous, and Metastatic Cells Using Conjugated Fluorescent Polymers. *J. Am. Chem. Soc.* **2009**, *132*, 1018–1022.

(25) Bunz, U. H.; Rotello, V. M. Gold Nanoparticle–Fluorophore Complexes: Sensitive and Discerning “Noses” for Biosystems Sensing. *Angew. Chem., Int. Ed.* **2010**, *49*, 3268–3279.

(26) You, C.-C.; Miranda, O. R.; Gider, B.; Ghosh, P. S.; Kim, I.-B.; Erdogan, B.; Krovi, S. A.; Bunz, U. H.; Rotello, V. M. Detection and Identification of Proteins Using Nanoparticle–Fluorescent Polymer ‘Chemical Nose’ Sensors. *Nat. Nanotechnol.* **2007**, *2*, 318–323.

(27) De, M.; Rana, S.; Akpınar, H.; Miranda, O. R.; Arvizo, R. R.; Bunz, U. H.; Rotello, V. M. Sensing of Proteins in Human Serum Using Conjugates of Nanoparticles and Green Fluorescent Protein. *Nat. Chem.* **2009**, *1*, 461–465.

(28) Phillips, R. L.; Miranda, O. R.; You, C. C.; Rotello, V. M.; Bunz, U. H. Rapid and Efficient Identification of Bacteria Using Gold-Nanoparticle-Poly(*para*-phenyleneethynylene) Constructs. *Angew. Chem., Int. Ed.* **2008**, *47*, 2590–2594.

(29) Bajaj, A.; Miranda, O. R.; Kim, I.-B.; Phillips, R. L.; Jerry, D. J.; Bunz, U. H.; Rotello, V. M. Detection and Differentiation of Normal, Cancerous, and Metastatic Cells Using Nanoparticle-Polymer Sensor Arrays. *Proc. Natl. Acad. Sci. U.S.A.* **2009**, *106*, 10912.

(30) Bunz, U. Poly(aryleneethynylene)s: Syntheses, Properties, Structures, and Applications. *Chem. Rev.* **2000**, *100*, 1605–1644.

(31) Zhao, X.; Pinto, M. R.; Hardison, L. M.; Mwaura, J.; Müller, J.; Jiang, H.; Witker, D.; Kleiman, V. D.; Reynolds, J. R.; Schanze, K. S. Variable Band Gap Poly(arylene ethynylene) Conjugated Polyelectrolytes. *Macromolecules* **2006**, *39*, 6355–6366.

(32) Shen, D.; Wang, L.; Pan, Z.; Cheng, S.; Zhu, X.; Fan, L. J. Toward a Highly Sensitive Fluorescence Sensing System of an Amphiphilic Molecular Rod: Facile Synthesis and Significant Solvent-Assisted Photophysical Tunability. *Macromolecules* **2011**, *44*, 1009–1015.

(33) Wang, S.; Zhao, W.; Song, J.; Cheng, S.; Fan, L. J. A Platform for Preparation of Monodispersed Fluorescent Conjugated Polymer Microspheres with Core-Shell Structures. *Macromol. Rapid Commun.* **2013**, *34*, 102–108.

- (34) Dickinson, T. A.; Walt, D. R.; White, J.; Kauer, J. S. Generating Sensor Diversity Through Combinatorial Polymer Synthesis. *Anal. Chem.* **1997**, *69*, 3413–3418.
- (35) Schiedel, M. S.; Briehn, C. A.; Bäuerle, P. Single-Compound Libraries of Organic Materials: Parallel Synthesis and Screening of Fluorescent Dyes. *Angew. Chem., Int. Ed.* **2001**, *40*, 4677–4680.
- (36) Rochat, S. b.; Severin, K. Pattern-Based Sensing with Metal–Dye Complexes: Sensor Arrays versus Dynamic Combinatorial Libraries. *J. Comb. Chem.* **2010**, *12*, 595–599.
- (37) Vendrell, M.; Zhai, D.; Er, J. C.; Chang, Y.-T. Combinatorial Strategies in Fluorescent Probe Development. *Chem. Rev.* **2012**, *112*, 4391–4420.
- (38) Fan, L. J.; Zhang, Y.; Jones, W. E. Design and Synthesis of Fluorescence “Turn-on” Chemosensors Based on Photoinduced Electron Transfer in Conjugated Polymers. *Macromolecules* **2005**, *38*, 2844–2849.
- (39) Fan, L. J.; Jones, W. E., Jr. Studies of Photoinduced Electron Transfer and Energy Migration in a Conjugated Polymer System for Fluorescence “Turn-on” Chemosensor Applications. *J. Phys. Chem. B* **2006**, *110*, 7777–7782.
- (40) Murphy, C. B.; Zhang, Y.; Troxler, T.; Ferry, V.; Martin, J. J.; Jones, W. E., Jr. Probing Förster and Dexter Energy-Transfer Mechanisms in Fluorescent Conjugated Polymer Chemosensors. *J. Phys. Chem. B* **2004**, *108*, 1537–1543.
- (41) Pang, Y.; Li, J.; Barton, T. J. Processible Poly(*p*-phenyleneethynylene)-*alt*-(2,5-thienyleneethynylene)s of High Luminescence: Their Synthesis and Physical Properties. *J. Mater. Chem.* **1998**, *8*, 1687–1690.
- (42) Swager, T. M.; Gil, C. J.; Wrighton, M. S. Fluorescence Studies of Poly(*p*-phenyleneethynylene)s: The Effect of Anthracene Substitution. *J. Phys. Chem.* **1995**, *99*, 4886–4893.
- (43) Mandal, S. S.; Chakraborty, J.; De, A. Studies in Sulfur Heterocycles. Part 15. Condensed Heterocycles Derived from Thieno[2,3-*c*]- and Thieno[3,2-*c*]-thiopyrans. *J. Chem. Soc., Perkin Trans. I* **1999**, 2639–2644.
- (44) Haskins-Glusac, K.; Pinto, M. R.; Tan, C.; Schanze, K. S. Luminescence Quenching of a Phosphorescent Conjugated Polyelectrolyte. *J. Am. Chem. Soc.* **2004**, *126*, 14964–14971.
- (45) Kim, I. B.; Dunkhorst, A.; Gilbert, J.; Bunz, U. H. F. Sensing of Lead Ions by a Carboxylate-Substituted PPE: Multivalency Effects. *Macromolecules* **2005**, *38*, 4560–4562.
- (46) Moroni, M.; Le Moigne, J.; Luzzati, S. Rigid Rod Conjugated Polymers for Nonlinear Optics: 1. Characterization and Linear Optical Properties of Poly(aryleneethynylene) Derivatives. *Macromolecules* **1994**, *27*, 562–571.
- (47) Zhang, Y.; Murphy, C. B.; Jones, W. E. Poly[*p*-(phenyleneethynylene)-*alt*-(thienyleneethynylene)] Polymers with Oligopyridine Pendant Groups: Highly Sensitive Chemosensors for Transition Metal Ions. *Macromolecules* **2001**, *35*, 630–636.
- (48) Jurs, P.; Bakken, G.; McClelland, H. Computational Methods for the Analysis of Chemical Sensor Array Data from Volatile Analytes. *Chem. Rev.* **2000**, *100*, 2649–2678.